

High-Silica Zeolite SSZ-61 with Dumbbell-Shaped Extra-Large-Pore Channels**

Stef Smeets, Dan Xie,* Christian Baerlocher, Lynne B. McCusker,* Wei Wan, Xiaodong Zou, and Stacey I. Zones

Abstract: The synthesis of the high-silica zeolite SSZ-61 using a particularly bulky polycyclic structure-directing agent and the subsequent elucidation of its unusual framework structure with extra-large dumbbell-shaped pore openings are described. By using information derived from a variety of X-ray powder diffraction and electron microscopy techniques, the complex framework structure, with 20 Si atoms in the asymmetric unit, could be determined and the full structure refined. The Si atoms at the waist of the dumbbell are only three-connected and are bonded to terminal O atoms pointing into the channel. Unlike the six previously reported extra-large-pore zeolites, SSZ-61 contains no heteroatoms in the framework and can be calcined easily. This, coupled with the possibility of inserting a catalytically active center in the channel between the terminal O atoms in place of H^+ , afford SSZ-61 intriguing potential for catalytic applications.

Zeolites are crystalline aluminosilicate framework materials with pores of molecular dimensions. It is the variability in the structures of their well-defined pore systems that makes them so attractive as shape-selective catalysts. A zeolite is typically synthesized hydrothermally in the presence of an organic cation, around which the aluminosilicate framework forms.

Consequently, considerable effort has gone into creating novel organic cations, also called structure-directing agents (SDAs), with the hope that they, in turn, will help to direct the formation of novel host frameworks.^[1] Larger SDAs that are still soluble in water, for example, might promote the formation of zeolites with larger pores. If the crystallized framework is an aluminosilicate, the SDA can usually be removed easily by heat treatment leaving the porous framework structure intact. In what follows, we describe the synthesis of high-silica SSZ-61 using a particularly bulky polycyclic SDA (Figure 1 a), and the challenges that had to be overcome to elucidate its unusual structure.

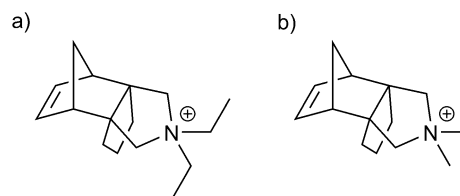


Figure 1. SDA used in the synthesis of a) SSZ-61 (8-azonia-8,8-diethyltetracyclo[4.3.3.1^{2,5}.0^{1,6}]tridec-3-ene), and b) SSZ-35 (8-azonia-8,8-dimethyltetracyclo[4.3.3.1^{2,5}.0^{1,6}]tridec-3-ene).

An SDA is usually a quaternary ammonium compound that is stable at elevated temperatures,^[2] although phosphonium cations have also been used.^[3,4] In the past we have found it helpful to create families of SDAs built around a particular organic entity. For example, using a Diels–Alder strategy, Nakagawa brought together sources of reactive dienes and dienophiles to build the skeleton of a polycyclic hydrocarbon with some rigidity (Figure S1a in the Supporting Information). This could then be transformed into a family of organic cations that produced a series of different zeolites.^[5] Later, another layer of complexity was added to increase the size of the SDA by using a bicyclic dienophile in the reaction (Figure S1b). The variant with two *N*-Methyl groups shown in Figure 1 b has been found to be particularly selective for the zeolite SSZ-35^[6] (framework type **STF**^[7,8]), and its excellent pore-filling function was confirmed by molecular modeling.^[9]

If one or both of the *N*-methyl groups is replaced with the next largest candidate, ethyl, a new material, SSZ-61, emerges, albeit under a much narrower set of hydrothermal synthesis conditions than those found for SSZ-35. The synthesis was performed in relatively dilute conditions using fluoride rather than hydroxide as the mineralizer.^[10–12] With this fluoride route, high reactant concentrations, where the Si–F interaction is significant, tend to produce multi-dimen-

[*] S. Smeets, Dr. D. Xie, Dr. C. Baerlocher, Dr. L. B. McCusker
Laboratory of Crystallography, ETH Zurich
8093 Zurich (Switzerland)
E-mail: mccusker@mat.ethz.ch

Dr. D. Xie, Dr. S. I. Zones
Chevron Energy Technology Company
Richmond, CA 94802 (USA)
E-mail: dan.xie@chevron.com

Dr. W. Wan, Prof. X. Zou
Inorganic and Structural Chemistry
Department of Materials and Environmental Chemistry
Stockholm University, 10691 Stockholm (Sweden)

[**] We thank the beamline scientists on the Swiss Norwegian Beamlines at the European Synchrotron Radiation Facility in Grenoble, France and on the Materials Science Beamline at the SLS in Villigen, Switzerland for their assistance with the powder diffraction measurements, Sonjong Hwang (CalTech) for the NMR analysis, and Cong-Yan Chen (Chevron) for the initial adsorption experiments. S.I.Z. thanks Michael Tsapatsis (University of Minnesota) for his early interest in this material. This work was supported by the Swiss National Science Foundation, the Chevron Energy Technology Company, and the Swedish Research Council (VR) and the Knut and Alice Wallenberg Foundation through the 3DEM-NATUR project. The EM facility was supported by the Knut and Alice Wallenberg Foundation.

Supporting information for this article is available on the WWW under <http://dx.doi.org/10.1002/ange.201405658>.

sional channel systems. In more dilute systems, where the structure-directing influence of the fluoride is diminished, one-dimensional channel systems and higher framework densities are favored.^[13] It is under the latter conditions that SSZ-61 was synthesized,^[14,15] and its structure indeed proved to be consistent with these trends.

For most applications, the organic guest species are first removed from the zeolite by calcination at ca. 300–600 °C, leaving behind a porous host. Synchrotron X-ray powder diffraction (XPD) data were collected on a sample of SSZ-61 that had been calcined in this way, but because the crystallites of SSZ-61 are very fine needles (ca. 100 nm thick, Figure 2),

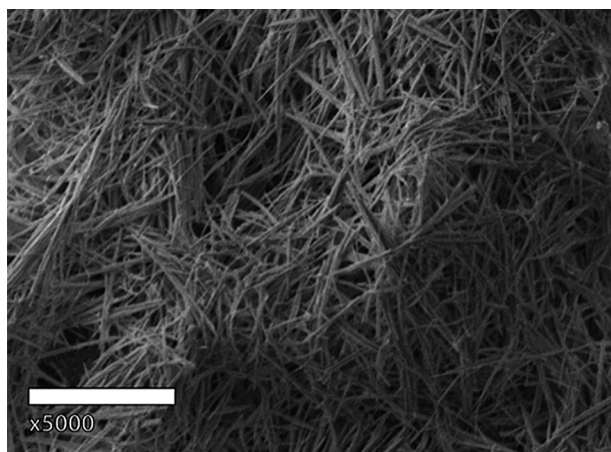


Figure 2. Scanning electron microscopy image showing the morphology of SSZ-61. The scale bar is 5 μm.

most diffraction peaks are broadened and the pattern was of poor quality (Figure S2). Initial attempts to index the pattern failed, but by using these data in conjunction with electron diffraction data collected along different projections, a *C*-centred monoclinic unit cell ($a = 25.03 \text{ Å}$, $b = 5.30 \text{ Å}$, $c = 19.99 \text{ Å}$, $\beta = 104.5^\circ$) could be derived.

The short repeat distance along *b* indicated that SSZ-61 was likely to have a one-dimensional channel system in that direction, in line with expectations emanating from the synthesis conditions. A further transmission electron microscopy experiment showed that this short axis was aligned with the needle axis of the SSZ-61 crystal. It was also noted that the *a* and *b* parameters were very similar to those of the framework types **MTW** ($C2/m$; $a = 25.6 \text{ Å}$, $b = 5.3 \text{ Å}$, $c = 12.1 \text{ Å}$, $\beta = 109.3^\circ$) and **SFN** ($C2/m$; $a = 25.2 \text{ Å}$, $b = 5.3 \text{ Å}$, $c = 15.0 \text{ Å}$, $\beta = 103.9^\circ$), which are closely related to one another. **SFN** can be described as a sigma expansion of **MTW** (Figure S3).^[16]

Through-focus high-resolution transmission electron microscopy (HRTEM) images along different zone axes, each series containing 20 images with fixed focus intervals, were then collected. Structure projections were reconstructed from the through-focus HRTEM images by compensating for the effects of contrast transfer functions (CTFs) of the microscope lenses and combining CTF-corrected images.^[17] Unfortunately, images along the channel direction (i.e.,

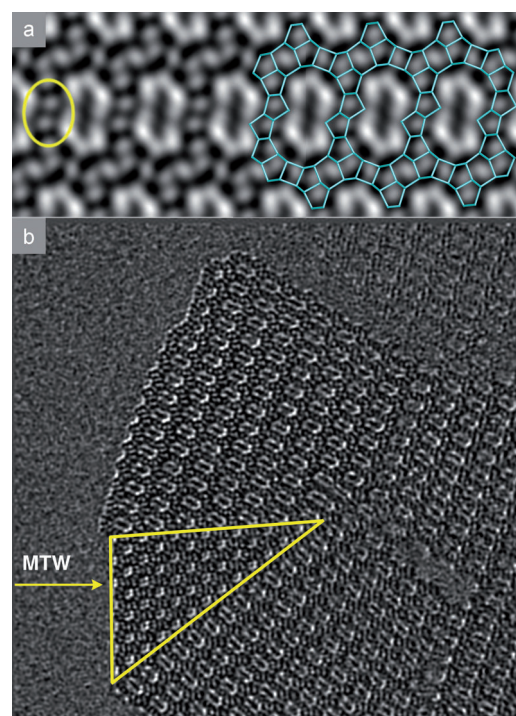


Figure 3. Images of SSZ-61 reconstructed from a series of through-focus HRTEM images. a) Lattice averaged image viewed along the channel direction highlighting the connecting rings (yellow) and a possible arrangement (blue) of 4-, 5- and 6-rings around the large pore. b) Image showing an **MTW**-type intergrowth (yellow triangle).

down the needle axis) could not be obtained at first, so the ultra-microtome technique was used to prepare suitable samples. The resulting reconstructed images showed a large elongated pore delimited by 4-, 5- and 6-rings very clearly (Figure 3a). Furthermore, intergrowths of a 12-ring structure (possibly **MTW**-type) could be identified (Figure 3b). With this information, it was then possible to construct a framework model for SSZ-61 with the layers common to **SFN** and **MTW** connected by pairs of 5-rings to create a dumbbell-shaped 18-ring pore (model A; Figure 4a). The 5-rings connect down the channel (parallel to the *b* axis) to form triple zigzag chains. Unfortunately, this model contains a significant number of Si atoms that are only two-connected (rather than four-connected), and this is inconsistent with ^{29}Si MAS NMR measurements, which revealed the presence of an unusually large percentage of three-connected (Q^3) Si atoms, with a $\text{Q}^3:\text{Q}^4$ ratio of 1:5, but no Q^2 Si atoms.

The early reconstructed HRTEM images showed a faint line of contrast across the “waist” of the channels, which could be because of truncation effects in the imaging, but could also come from the structure. Therefore, model A was modified to include a bridge of two T atoms across the channels, thereby creating two 12-rings, eliminating the Q^2 Si atoms and forming Q^3 Si atoms (model B; Figure 4b). The geometry of this model could be optimized with a distance least-squares (DLS) refinement,^[18] showing it to be intrinsically robust, and the calculated XPD pattern looked promising.

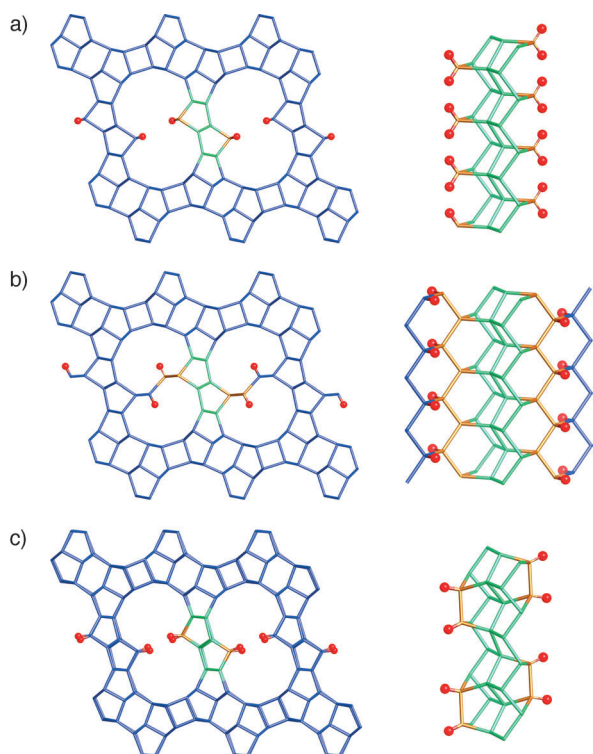


Figure 4. Structural models for SSZ-61. a) Model A with Q^2 Si atoms, b) model B with two 12-ring channels, and c) model C with 18-ring dumbbell-shaped channels. In each case, the [010] projection is shown on the left, and the connecting chain down the channel on the right. The triple zigzag chain is shown in green and the different connections are highlighted in orange. Model C proved to be the correct one. Bridging O atoms have been omitted for clarity.

In an attempt to obtain better quality XPD data, synchrotron data were collected on an as-synthesized sample of SSZ-61. This pattern was indeed better, though still not good (Figure S4), and could be indexed directly using the auto-indexing procedure in the program *Topas*^[19] (*C*-centered; $a = 25.2370 \text{ \AA}$, $b = 5.0367 \text{ \AA}$, $c = 19.7500 \text{ \AA}$, $\beta = 106.9^\circ$).

Unfortunately, Rietveld refinement^[20] of model B described above did not converge. Furthermore, it became apparent that there was not enough space in the 12-ring channels with the terminal O atom protruding into the channel to accommodate the bulky organic SDA, so the model was modified once again. The connection across the channel was removed to allow more space for the SDA, and the problematic Q^2 Si atoms in model A were connected to one another directly in a pairwise fashion along the channel wall (model C; Figure 4c). In this way, the two-connected Si atoms became three-connected. This adjustment required that the b axis be doubled, the space group changed to $P2_1/c$, the number of Si atoms per asymmetric unit be increased to 20, and the unit cell axes switched ($a = 19.8 \text{ \AA}$, $b = 10.1 \text{ \AA}$, $c = 25.2 \text{ \AA}$, $\beta = 106.9^\circ$).

With the DLS-optimized coordinates for model C, structure refinement using the Rietveld method as implemented in *Topas*^[21] was started. Despite the mediocre quality of the diffraction pattern, a difference electron density map gen-

erated using just the framework structure showed clouds of density within the pores of the zeolite, presumably indicating the location of the SDA. Therefore, an idealized model of the SDA was added to the refinement as a rigid body and its initial location and orientation were found by applying the simulated annealing routine in *Topas*. It was then converted to a flexible model with geometric restraints for further refinement.

The three-dimensional framework structure of SSZ-61 is characterized by large 1-dimensional, dumbbell-shaped, 18-ring channels running along the [010] direction (Figure 5).

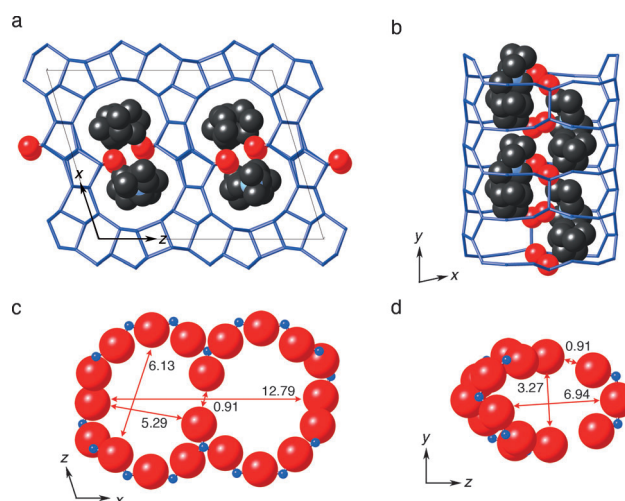


Figure 5. Framework structure of SSZ-61 showing the 18-ring channels and the location of the SDAs viewed a) down the channel and b) from the side. The terminal O atoms are shown in red and other O and H atoms have been omitted for clarity. Details of the effective pore openings of c) the 18-ring and d) the window across the waist of the 18-ring. All O–O distances shown are in Ångstrom and the O radius of 1.35 Å has been subtracted.

Si atoms at the waist of the channel are only three-connected and are bonded to terminal O atoms pointing into the channel. The free distance between these terminal O atoms across the channel is less than 1 Å (assuming an oxygen radius of 1.35 Å). The effective pore openings of the two rings that form the dumbbell (each defined by 11 O atoms) are approximately $5.3 \text{ \AA} \times 6.1 \text{ \AA}$ (Figure 5c). Along the [100] direction, the terminal O atoms form what could be viewed as a window between the two halves of the channel, with an effective opening of $6.9 \text{ \AA} \times 3.3 \text{ \AA}$ (Figure 5d).

The framework structure is closely related to those of ZSM-12 (**MTW**)^[22] and SSZ-59 (**SFN**)^[23]. All three have the same layers; they differ only in the connection between these layers. In **MTW** the layers are connected directly, creating single zigzag chains running down the sides of the 12-ring channel. In **SFN** the layers are separated by 4-rings, which increases the c axis by 2.9 Å and creates a 14-ring channel with double zigzag chains. In SSZ-61, the connection is via two 5-rings, extending the axis by 7.7 Å and creating an 18-ring channel with triple zigzag chains. The three chains are linked in an alternating fashion to form a series of 6-rings, and the 6-rings are spanned in turn by an additional Si atom to

form two 5-rings, and these Si atoms are linked pairwise to form *mor* units^[24] on both sides of the chains (Figure 4c).

Each half of the 18-ring channel in SSZ-61 contains one SDA cation to give a total of four per unit cell (Figure 5). The dumbbell-shaped pore provides room for the bulky part of the SDA, and allows the positively charged N atom to lie near two terminal O atoms. As in the case of SSZ-35, the framework wraps tightly around the SDA, but in this case it wraps around pairs of the organic cations. Of the 80 Si atoms per unit cell in SSZ-61, eight are only three-connected, which is less than the 13 Q³ Si atoms per unit cell expected on the basis of the NMR data. We assume that the additional Q³ Si atoms arise from defects in the material. The fourth bond of these Q³ Si atoms is to a terminal O atom that protrudes into the 18-ring channel. From charge balance considerations, it is likely that four of the eight terminal O atoms are protonated and that the four organic cations compensate for the charge on the other four.

Although the HRTEM images show evidence of stacking disorder in SSZ-61 (Figure 3b and S7), *DIFFaX*^[25] simulations of different degrees of faulting (Figure S8) indicate that the level is below 5%. The fact that no reflections with odd *k* (i.e. those requiring the doubled *b* axis, Figure S9) were observed in 3-dimensional rotation electron diffraction (RED) data,^[26] prompted us to re-examine the structural model. A second potential source of disorder involving the Q³ Si atoms was found. These Si atoms are linked along the channel in a pairwise fashion, and two pairing arrangements are possible (Figure S10). To model this disorder, four Si and ten O atom positions were split and a second (constrained) position and orientation of the SDA was added to the model. All were assigned occupancies of 0.5. With this model, the profile fit in the 5–10°2 θ region improved considerably (Figure S11) and refinement converged with $R_F = 0.070$ and $R_{wp} = 0.110$ ($R_{exp} = 0.103$). In the ordered structure, the pairs of Q³ Si atoms in adjacent 18-rings are strictly alternating in an up-down arrangement, but in fact, an up-up or down-down sequence is equally probable. Fortunately, the 18-ring channel is not affected at all by this minor disorder. More details of the refinement and the disorder are given in the Supplementary Information.

Initial adsorption experiments have been taken for SSZ-61 using 2,2-dimethyl butane (kinetic diameter = 6.2 Å) and 1,3,5-triisopropylbenzene (kinetic diameter = 8.5 Å) as adsorbates. It is not surprising that SSZ-61 can take up 2,2-dimethyl butane as does **MTW** and other 12-ring zeolites like SSZ-24 (**AFI**).^[27] But there is also some evidence of slow, diffusion-hindered uptake of the planar adsorbate, 1,3,5-triisopropylbenzene. This adsorbate was used to give the first indication that the zeolite UTD-1 (**DON**) might be an extra-large pore zeolite (it was eventually shown to be a one-dimensional 14-ring zeolite), because the larger adsorbate yielded the same pore filling as the 2,2-dimethyl butane. Other 12-ring zeolites only show filling by the latter.^[28] A more open framework material VPI-5 (**VFI**, one-dimensional 18-ring aluminophosphate) shows equal filling for both adsorbates with no diffusion hindrance.^[28] SSZ-61 does not show equivalent filling for the two adsorbates but there is some very slow uptake of the larger one. The amount observed is above that

for the more hindered 14-ring zeolite CIT-5 (**CFI**) but smaller than that for SSZ-59 (**SFN**).^[23] so there must be some “breathing” of the SSZ-61 structure that allows the planar adsorbate a chance to pass through the narrow space at the center of the pore.

By combining several modern structure analysis techniques with zeolite crystal chemistry, the unusual structure of SSZ-61 could be elucidated. Not only the complex interrupted framework structure with 20 Si atoms in the asymmetric unit (24 in the disordered model), but also the location of the SDA within the pores of the zeolite could be clarified, despite the relatively poor quality of the powder diffraction pattern. Zeolites with 18-ring or larger pore openings are rare. To date only six have been reported and SSZ-61 makes the seventh. However, SSZ-61 is the first high-silica member of this family. All others are gallo- (**-CLO**) or aluminophosphates (**VFI**) or gallo- (**ETR**) or germanosilicates (**IRR**, **ITT**, **ITV**), which are difficult to calcine, especially in moist environments, and therefore less useful for application. While the 18-ring in SSZ-61 has a narrow waist that limits the size of molecule that can be adsorbed, precisely this waist offers the tantalizing possibility of inserting a catalytically active center in the channel between terminal O atoms in place of H⁺.

Further details on the crystal structure investigations for SSZ-61 may be obtained from the Fachinformationszentrum Karlsruhe, 76344 Eggenstein-Leopoldshafen, Germany (fax: (+49) 7247-808-666; e-mail: crysdata@fiz-karlsruhe.de), on quoting the depository number CSD-428025.

Received: May 26, 2014

Revised: July 3, 2014

Published online: August 1, 2014

Keywords: electron microscopy · microporous materials · structure elucidation · X-ray diffraction · zeolites

- [1] M. E. Davis, *Chem. Mater.* **2014**, 26, 239–245.
- [2] A. Corma, M. E. Davis, *ChemPhysChem* **2004**, 5, 304–313.
- [3] R. Simancas, D. Dari, N. Velamazán, M. T. Navarro, A. Cantin, G. Sastre, A. Corma, F. Rey, *Science* **2010**, 330, 1219–1222.
- [4] R. Simancas, J. L. Jorda, F. Rey, A. Corma, A. Cantin, I. Peral, C. Popescu, *J. Am. Chem. Soc.* **2014**, 136, 3342–3345.
- [5] Y. Nakagawa, S. I. Zones in *Synthesis of Microporous Materials I* (Eds.: M. L. Occelli, H. Robson), Van Nostrand Reinhold, New York, **1992**, pp. 373–383.
- [6] P. Wagner, Y. Nakagawa, G. S. Lee, M. E. Davis, S. Elomar, R. C. Medrud, S. I. Zones, *J. Am. Chem. Soc.* **2000**, 122, 263–273.
- [7] Three-letter framework type codes (boldface capital letters) for all zeolites mentioned in the text are given in parentheses.
- [8] C. Baerlocher, L. B. McCusker, D. H. Olson, *Atlas of Zeolite Framework Types*, Elsevier, Amsterdam, **2007** and <http://www.iza-structure.org/databases/>.
- [9] A. W. Burton, G. S. Lee, S. I. Zones, *Microporous Mesoporous Mater.* **2006**, 90, 129–144.
- [10] E. M. Flanigen, R. L. Patton, U.S. Patent 4,257,885, **1978**.
- [11] J. L. Guth, H. Kessler, R. Wey in *Proc. 7th Int. Zeolite Conf.* (Eds.: Y. Murakami, A. Iijima, J. W. Ward), Kodansha, Tokyo, **1986**, pp. 121–128.
- [12] M. A. Camblor, L. A. Villaescusa, M. J. Díaz-Cabañas, *Top. Catal.* **1999**, 9, 59–76.

- [13] S. I. Zones, A. W. Burton, G. S. Lee, M. M. Olmstead, *J. Am. Chem. Soc.* **2007**, *129*, 9066–9079.
- [14] S. I. Zones, S. Elomari, U.S. Patent 6,929,789, **2005**.
- [15] S. I. Zones, S. J. Hwang, S. Elomari, I. Ogino, M. E. Davis, A. W. Burton, *C. R. Chim.* **2005**, *8*, 267–282.
- [16] D. P. Shoemaker in *Proc. 3rd. Int. Conf. Molecular Sieves* (Ed.: J. B. Uytterhoeven, Leuven University Press, Leuven, **1973**, pp. 138–143.
- [17] W. Wan, S. Hovmöller, X. D. Zou, *Ultramicroscopy* **2012**, *115*, 50–60.
- [18] C. Baerlocher, A. Hepp, W. M. Meier, *DLS-76, a program for the simulation of crystal structures by geometric refinement*, Institute of Crystallography and Petrography, ETH Zurich, **1977**.
- [19] A. A. Coelho, *J. Appl. Crystallogr.* **2003**, *36*, 86–95.
- [20] H. M. Rietveld, *J. Appl. Crystallogr.* **1969**, *2*, 65–71.
- [21] A. A. Coelho, *TOPAS-ACADEMIC* v4.1., **2007**.
- [22] R. B. LaPierre, Jr., A. C. R. Rohrman, J. L. Schlenker, J. D. Wood, M. K. Rubin, W. J. Rohrbaugh, *Zeolites* **1985**, *5*, 346–348.
- [23] A. Burton, S. Elomari, C. Y. Chen, R. C. Medrud, I. Y. Chan, L. M. Bull, C. Kibby, T. V. Harris, S. I. Zones, E. S. Vittoratos, *Chem. Eur. J.* **2003**, *9*, 5737–5748.
- [24] Composite building units found in more than one framework type have been assigned three letter codes (*italic small letters*), which are listed in Ref. [7]. The *mor* unit is found in 25 different framework types.
- [25] M. M. J. Treacy, J. M. Newsam, M. W. Deem, *Proc. R. Soc. London Ser. A* **1991**, *433*, 499–520.
- [26] W. Wan, J. L. Sun, J. Su, S. Hovmöller, X. D. Zou, *J. Appl. Crystallogr.* **2013**, *46*, 1863–1873.
- [27] M. Yoshikawa, P. Wagner, M. Lovallo, T. Takewaki, C. Y. Chen, L. W. Beck, C. Jones, M. Tsapatsis, S. I. Zones, M. E. Davis, *J. Phys. Chem. B* **1998**, *102*, 7139–7147.
- [28] R. F. Lobo, M. Tsapatsis, C. C. Freyhardt, S. Khodabandeh, P. Wagner, C. Y. Chen, K. Balkus, S. I. Zones, M. E. Davis, *J. Am. Chem. Soc.* **1997**, *119*, 8474–8484.